Quantum effects in photon emission by electron wave packets in (magnetic fields and) matter

Dmitry Karlovets

ITMO University, St. Petersburg

18.12.2024

d.karlovets@gmail.com

SYSU, Zhuhai

Outline

1. An r-t/phase-space approach in photon emission
2. Example: Cherenkov radiation and its Wigner function
3. Photon field dynamics at a finite distance:
    - The photon spreading time
    - The Mach cone formation
    - The photon arrival time and its quantum shift
4. Summary and Outlook

Based on arxiv: 2411.00212

The problem

The r-t description of particle interactions in QFT is challenging,

but sometimes unavoidable:

- Collisions of beams at large impact parameters,
- Collisions of non-Gaussian packets (say, the vortex particles)
- Neutrino oscillations,
- Near-field, formation zone, pre-wave zone effects in radiation and scattering,
- Generalized measurements and entanglement in collisions,
- Studying process dynamics in real space and time,

and so on

R-t approach to photon emission

An S-matrix within the 1st order of the perturbation theory:

$$\hat{S} \approx \hat{1} + \hat{S}^{(1)} = \hat{1} - ie \int d^4x \, \hat{j}^{\mu}(x) \hat{A}_{\mu}(x),$$

An evolved state in the photon emission:

$$|e', \gamma\rangle = \left(\hat{1} + \hat{S}^{(1)}\right) |\text{in}\rangle,$$

$$|e', \gamma\rangle = |\text{in}\rangle + \sum_{\lambda'=\pm 1/2, \lambda_\gamma = \pm 1} \int \frac{d^3k}{(2\pi)^3} \frac{d^3p'}{(2\pi)^3} |\mathbf{p}', \lambda'\rangle \otimes |\mathbf{k}, \lambda_\gamma\rangle \, S_{fi}^{(1)}$$

If the electron is detected as a plane wave, the photon states becomes:

$$|\gamma\rangle = \langle \mathbf{p}', \lambda' | e_{\text{in}} \rangle |0_\gamma\rangle + \sum_{\lambda_\gamma} \int \frac{d^3k}{(2\pi)^3} |\mathbf{k}, \lambda_\gamma\rangle \, S_{fi}^{(1)},$$

Field operators:

$$\hat{\boldsymbol{E}}(\boldsymbol{r},t) = -\frac{\partial \hat{\boldsymbol{A}}(\boldsymbol{r},t)}{\partial t} = \sum_{\lambda_\gamma=\pm 1} \int \frac{d^3k}{(2\pi)^3}\, i\omega \left(\boldsymbol{A}_{\boldsymbol{k}\lambda_\gamma}(\boldsymbol{r},t)\, \hat{c}_{\boldsymbol{k}\lambda_\gamma} - \text{h.c.} \right), \boldsymbol{A}_{\boldsymbol{k}\lambda_\gamma}(\boldsymbol{r},t) = \frac{\sqrt{4\pi}}{\sqrt{2\omega}}\, \boldsymbol{e}_{\boldsymbol{k}\lambda_\gamma}\, e^{-i\omega t + i\boldsymbol{k}\cdot\boldsymbol{r}},$$

Energy density:

$$\mathcal{W}(\mathrm{r},t) = \frac{1}{8\pi}\langle\gamma|\hat{\boldsymbol{E}}^2(\boldsymbol{r},t) + \hat{\boldsymbol{H}}^2(\boldsymbol{r},t)|\gamma\rangle - \frac{\varepsilon_0}{4\pi} = \frac{1}{4\pi}\left(\left|\langle 0|\hat{\boldsymbol{E}}(\boldsymbol{r},t)|\gamma\rangle\right|^2 + \left|\langle 0|\hat{\boldsymbol{H}}(\boldsymbol{r},t)|\gamma\rangle\right|^2 \right)$$

$$\langle 0|\hat{\boldsymbol{E}}(\boldsymbol{r},t)|\gamma\rangle = \sum_{\lambda_\gamma} \int \frac{d^3k}{(2\pi)^3} i\omega \boldsymbol{A}_{\boldsymbol{k}\lambda_\gamma}(\boldsymbol{r},t)\, S^{(1)}_{fi}(\mathrm{k},\lambda_\gamma),$$

A vacuum contribution:

$$\varepsilon_0 = \langle\gamma|\gamma\rangle \sum_{\lambda_\gamma} \int \frac{d^3k}{(2\pi)^3}\, \omega^2 |\boldsymbol{A}_{\boldsymbol{k}\lambda_\gamma}(\boldsymbol{r},t)|^2 = \langle\gamma|\gamma\rangle \sum_{\lambda_\gamma} \int \frac{d^3k}{(2\pi)^3}\, 2\pi\omega$$

Energy density:

$$\frac{1}{4\pi}\left|\langle 0|\hat{\boldsymbol{E}}(r,t)|\gamma\rangle\right|^2 = \frac{1}{4\pi}\left|\sum_{\lambda_\gamma}\int \frac{d^3k}{(2\pi)^3}\,\boldsymbol{E}_{\lambda_\gamma}(\mathrm{k})\,e^{-ikx}\right|^2 =$$

$$= \frac{1}{4\pi}\sum_{\lambda_\gamma,\tilde{\lambda}_\gamma}\int \frac{d^3k}{(2\pi)^3}\frac{d^3\tilde{k}}{(2\pi)^3}\,\boldsymbol{E}^*_{\tilde{\lambda}_\gamma}(\mathrm{k}-\tilde{\mathrm{k}}/2)\cdot\boldsymbol{E}_{\lambda_\gamma}(\mathrm{k}+\tilde{\mathrm{k}}/2)\,e^{-it\left(\omega(\mathrm{k}+\tilde{\mathrm{k}}/2)-\omega(\mathrm{k}-\tilde{\mathrm{k}}/2)\right)+i\mathrm{r}\cdot\tilde{\mathrm{k}}} \equiv$$

$$\equiv \int \frac{d^3k}{(2\pi)^3}\,\mathcal{W}(\mathrm{r},\mathrm{k},t), \qquad \text{The 1st marginal distribution}$$

$$\boldsymbol{E}_{\lambda_\gamma}(\mathrm{k}) = \frac{i\omega\sqrt{4\pi}}{\sqrt{2\omega n^2}}\,\boldsymbol{e}_{\mathrm{k}\lambda_\gamma}\sum_{\lambda}\int \frac{d^3p}{(2\pi)^3}\,f_e^{(\mathrm{in})}(\mathrm{p},\lambda)S_{fi}^{(1)}(\mathrm{p},\lambda,\mathrm{k},\lambda_\gamma)$$

The wave function of the incoming electron:

$$f_e^{(\mathrm{in})}(\mathrm{p},\lambda) = \langle \mathrm{p},\lambda|e_{\mathrm{in}}\rangle = \delta_{\lambda,\lambda_e}\left(\frac{2\sqrt{\pi}}{\sigma}\right)^{3/2}\exp\left\{-\frac{(\mathrm{p}-\langle\mathrm{p}\rangle)^2}{2\sigma^2}\right\},$$

The Wigner function:

$$\mathcal{W}(\mathbf{r},\mathbf{k},t)=\frac{1}{4\pi}\sum_{\lambda_\gamma,\tilde{\lambda}_\gamma}\int\frac{d^3\tilde{k}}{(2\pi)^3}\,\boldsymbol{E}^*_{\tilde{\lambda}_\gamma}(\mathbf{k}-\tilde{\mathbf{k}}/2)\cdot\boldsymbol{E}_{\lambda_\gamma}(\mathbf{k}+\tilde{\mathbf{k}}/2)\,e^{-it\left(\omega(\mathbf{k}+\tilde{\mathbf{k}}/2)-\omega(\mathbf{k}-\tilde{\mathbf{k}}/2)\right)+i\mathbf{r}\cdot\tilde{\mathbf{k}}},$$

The photon field in phase space:
more information than we get from

the 2nd marginal distribution:

$$\int d^3x\,\mathcal{W}(\mathbf{r},\mathbf{k},t)\propto|S_{fi}(\langle\mathbf{p}\rangle,\lambda_e,\mathbf{k},\lambda_\gamma)|^2$$

No phase, not r-t

$$\int d^3x\,\mathcal{W}(\mathbf{r},\mathbf{k},t)=\frac{\omega}{2n^2}\left|\sum_\lambda\int\frac{d^3p}{(2\pi)^3}\,f_e^{(\mathrm{in})}(\mathbf{p},\lambda)S_{fi}(\mathbf{p},\lambda,\mathbf{k},\lambda_\gamma)\right|^2=$$

$$=\frac{\omega}{2n^2}(2\pi)^2\frac{T}{2\pi}\delta(\varepsilon(\mathbf{p})-\varepsilon'(\mathbf{p}')-\omega(\mathbf{k}))\,\frac{4\pi}{2\omega(\mathbf{k})n^2(\omega(\mathbf{k}))2\varepsilon(\mathbf{p})2\varepsilon'(\mathbf{p}')}\left|\sum_\lambda f_e^{(\mathrm{in})}(\mathbf{p},\lambda)\,M_{fi}(\mathbf{p},\mathbf{k},\lambda,\lambda_\gamma)\right|^2_{\mathbf{p}=\mathbf{p}'+\mathbf{k}}\qquad(17)$$

We calculate the Wigner function (***r***, ***k***, t) for Cherenkov radiation in the paraxial approximation:

The electron packet is narrow in momentum space: $\sigma \ll m$

The medium dispersion is weak: $\dfrac{\omega}{n(\omega)}\dfrac{dn(\omega)}{d\omega} \ll 1,$ $\mathrm{k}^2 = n^2(\omega)\omega^2$

The phase of the amplitude comes into play: ζ_{fi} $M_{fi}(\boldsymbol{p},\boldsymbol{k},\lambda_e,\lambda_\gamma) = |M_{fi}(\boldsymbol{p},\boldsymbol{k},\lambda_e,\lambda_\gamma)|\,\exp\{i\zeta_{fi}(\boldsymbol{p},\boldsymbol{k},\lambda_e,\lambda_\gamma)\}$

Cherenkov radiation in a transparent medium

$$M_{fi} = \sqrt{4\pi\alpha}\,\bar{u}_{\mathbf{p}'\lambda'}\gamma^{\mu}e^{*}_{\mu}u_{\mathbf{p}\lambda} = |M_{fi}|\,e^{i\zeta_{fi}},$$

$$u_{\mathbf{p}\lambda} = \sum_{\sigma=\pm 1/2} u^{(\sigma)}_{\varepsilon\lambda}\, d^{(1/2)}_{\sigma\lambda}(\theta)\, e^{-i\sigma\phi},$$

$$\bar{u}_{\mathbf{p}'\lambda'} = \sum_{\sigma'=\pm 1/2} \bar{u}^{(\sigma')}_{\varepsilon'\lambda'}\, d^{(1/2)}_{\sigma'\lambda'}(\theta')\, e^{i\sigma'\phi'},$$

$$e_{\mathbf{k}\lambda_\gamma} = \sum_{\sigma_\gamma=0,\pm 1} \chi^{(\sigma_\gamma)}\, d^{(1)}_{\sigma_\gamma\lambda_\gamma}(\theta_\gamma)\, e^{-i\sigma_\gamma\phi_\gamma}.$$

The amplitude phase is *not* vanishing even at the tree level:

$$M_{fi} = g_{\lambda\lambda'} \sum_{\sigma,\sigma',\sigma_\gamma} \delta_{\sigma,\sigma'+\sigma_\gamma}\, M^{(\sigma\sigma'\sigma_\gamma)}_{fi}\, e^{i\zeta^{(\sigma\sigma'\sigma_\gamma)}_{fi}} = g_{\lambda\lambda'}\Bigg(M^{(\frac{1}{2},-\frac{1}{2},1)}_{fi}\, e^{i\zeta^{(\frac{1}{2},-\frac{1}{2},1)}_{fi}} +$$

$$+ M^{(\frac{1}{2},\frac{1}{2},0)}_{fi}\, e^{i\zeta^{(\frac{1}{2},\frac{1}{2},0)}_{fi}} + M^{(-\frac{1}{2},\frac{1}{2},-1)}_{fi}\, e^{i\zeta^{(-\frac{1}{2},\frac{1}{2},-1)}_{fi}} + M^{(-\frac{1}{2},-\frac{1}{2},0)}_{fi}\, e^{i\zeta^{(-\frac{1}{2},-\frac{1}{2},0)}_{fi}} \Bigg),$$

$$\zeta_{fi} = \arctan \frac{\sum\limits_{\sigma,\sigma',\sigma_\gamma} \delta_{\sigma,\sigma'+\sigma_\gamma}\, M^{(\sigma\sigma'\sigma_\gamma)}_{fi} \sin\left(\zeta^{(\sigma\sigma'\sigma_\gamma)}_{fi}\right)}{\sum\limits_{\sigma,\sigma',\sigma_\gamma} \delta_{\sigma,\sigma'+\sigma_\gamma}\, M^{(\sigma\sigma'\sigma_\gamma)}_{fi} \cos\left(\zeta^{(\sigma\sigma'\sigma_\gamma)}_{fi}\right)},$$

The amplitude phase is non-vanishing *over a finite region of frequencies*, defined by the conservation laws

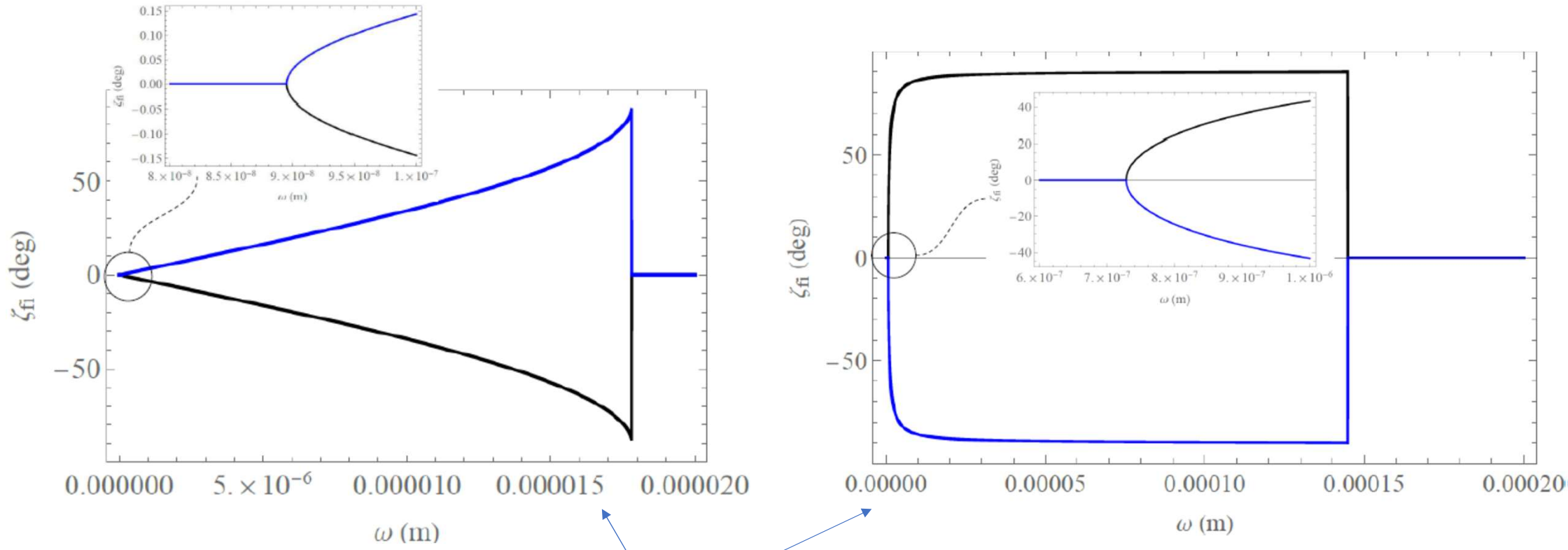

Figure 1: The phase of the scattering amplitude $\zeta_{fi} = \arg M_{fi}$ from Eq.(59) at the Cherenkov angle including the quantum recoil (44) for $\beta = 0.999$. Black line is for the first triangle point from Eq.(46), whereas the blue one is for the second point. Upper panel: $n = 1.5, p_\perp = 10^{-5}m, p'_\perp = 0.99 \times p_\perp, p'_z = 0.99 \times \beta, \lambda = \lambda' = 1/2, \lambda_\gamma = \pm 1$. Lower panel: $n = 1.7, p_\perp = 10^{-4}m, p'_\perp = 0.99 \times p_\perp, p'_z = 0.99 \times \beta, \lambda = -\lambda' = 1/2, \lambda_\gamma = \pm 1$. When $\lambda = -\lambda' = -1/2$, the black and blue lines swap.

The paraxial Wigner function is reduced to a 1D integral (akin to the retarded potentials):

$$\mathcal{W}_p(\mathbf{r},\mathbf{p},\mathbf{k},t) = \left(\frac{2\sqrt{\pi}}{\sigma}\right)^3 \frac{\sqrt{4\pi}}{(2n^2(\mathbf{k}))^2 2\varepsilon' 2\varepsilon(\mathbf{p})} \sum_{\lambda_\gamma} |M_{fi}(\mathbf{p},\lambda_e,\mathbf{k},\lambda_\gamma)|^2 \exp\left\{-\frac{(\mathbf{p}-\langle\mathbf{p}\rangle)^2}{\sigma^2}\right\}$$

$$\times \int_{-\infty}^{+\infty} \frac{dt'}{2\pi} \frac{1}{G(t')} \exp\left\{ it'(\varepsilon(\mathbf{p}) - \varepsilon' - \omega(\mathbf{k})) - \frac{i}{2} g(t') - \right.$$

$$\left. - \frac{1}{2\eta(t')} \frac{\eta(t')[\boldsymbol{R}\times(\boldsymbol{u}_p-\boldsymbol{u}_k)]^2 + \chi(t')(\boldsymbol{R}\cdot[\boldsymbol{u}_p\times\boldsymbol{u}_k])^2}{\eta(t')(\boldsymbol{u}_p-\boldsymbol{u}_k)^2 + \chi(t')\,[\boldsymbol{u}_p\times\boldsymbol{u}_k]^2} \right\}.$$

$$\boldsymbol{R} = \mathbf{r} - \boldsymbol{u}_p t + (\partial_{\mathbf{p}} + \partial_{\mathbf{k}})\zeta_{fi}(\mathbf{p},\lambda_e,\mathbf{k},\lambda_\gamma) \equiv$$
$$\equiv \{X,Y,Z\} = R\{\sin\theta_R\cos\phi_R, \sin\theta_R\sin\phi_R, \cos\theta_R\}$$

The group velocities of the Bohmian trajectories:

$$u_k = \frac{\partial \omega}{\partial \mathbf{k}} \approx \frac{\mathbf{k}}{n^2 \omega} = \frac{\mathbf{k}/|\mathbf{k}|}{n} \qquad u_p = \frac{\partial \varepsilon(\mathbf{p})}{\partial \mathbf{p}} = \frac{\mathbf{p}}{\varepsilon(\mathbf{p})},\ \varepsilon(\mathbf{p}) = \sqrt{m^2 + \mathbf{p}^2},$$

The photon Gouy phase due to spreading :

$$g(t') = g_1(t') + g_2(t')$$

$$g_1(t') = \arctan \frac{t'}{t_d},\ t_d = \frac{2}{\sigma^2} \frac{(\boldsymbol{u}_p - \boldsymbol{u}_k)^2}{\left(\frac{1}{\omega n^2} - \frac{1}{\varepsilon}\right)(\boldsymbol{u}_p - \boldsymbol{u}_k)^2 + \left(\frac{1}{\varepsilon} - \frac{1}{\omega}\right)[\boldsymbol{u}_p \times \boldsymbol{u}_k]^2},$$

$$g_2(t') = \arctan \frac{t'}{\tilde{t}_d},\ \tilde{t}_d = \frac{2}{\sigma^2} \frac{1}{\frac{1}{\omega n^2} - \frac{1}{\varepsilon}} = \frac{2}{\sigma^2} \frac{\omega n^2}{1 - n^2 \omega/\varepsilon}.$$

an effective spreading time

$$\tilde{t}_d = t_d(\theta = 0)$$

Most concisely:

$$\mathcal{W}(\mathbf{r},\mathbf{k},t) \propto \int_0^\infty dt' \, \frac{e^{-R^2/R_{\rm eff}^2(t')}}{G(t')} \cos\left(F(t')\right),$$

$$\boldsymbol{R} = \mathbf{r} - u_p t + (\partial_{\mathbf{p}} + \partial_{\mathbf{k}})\zeta_{fi}(\mathbf{p},\lambda_e,\mathbf{k},\lambda_\gamma)$$

a shift from the electron classical path
due to the medium polarization
and a finite free path of the virtual photon

This Wigner function:

1. Is *not* everywhere positive -- the «most quantum» feature,
2. If *not* for the phase, it would be concentrated around the classical path $r \sim u_p t$
3. It has an effective correlation length R_{eff}
4. It has the spreading time interval t_d and space region $\langle u \rangle t_d$ (formation length)

With the Wigner function, we can trace the spatio-temporal dynamics of the photon formation (phase-space tomography)

The classical Cherenkov angle (no quantum recoil)

$$\theta_{\mathrm{Ch.cl.}} = \arccos 1/u_p n$$

The quantum Cherenkov angle (with quantum recoil)

$$\cos\theta_{\mathrm{Ch}} = \frac{1}{\beta n} + \frac{\omega}{2\varepsilon}\frac{n^2-1}{\beta n},$$

The cut-off in the spectrum:

$$\omega_{\text{cut-off}} = 2\varepsilon\,\frac{\beta n - 1}{n^2 - 1},$$

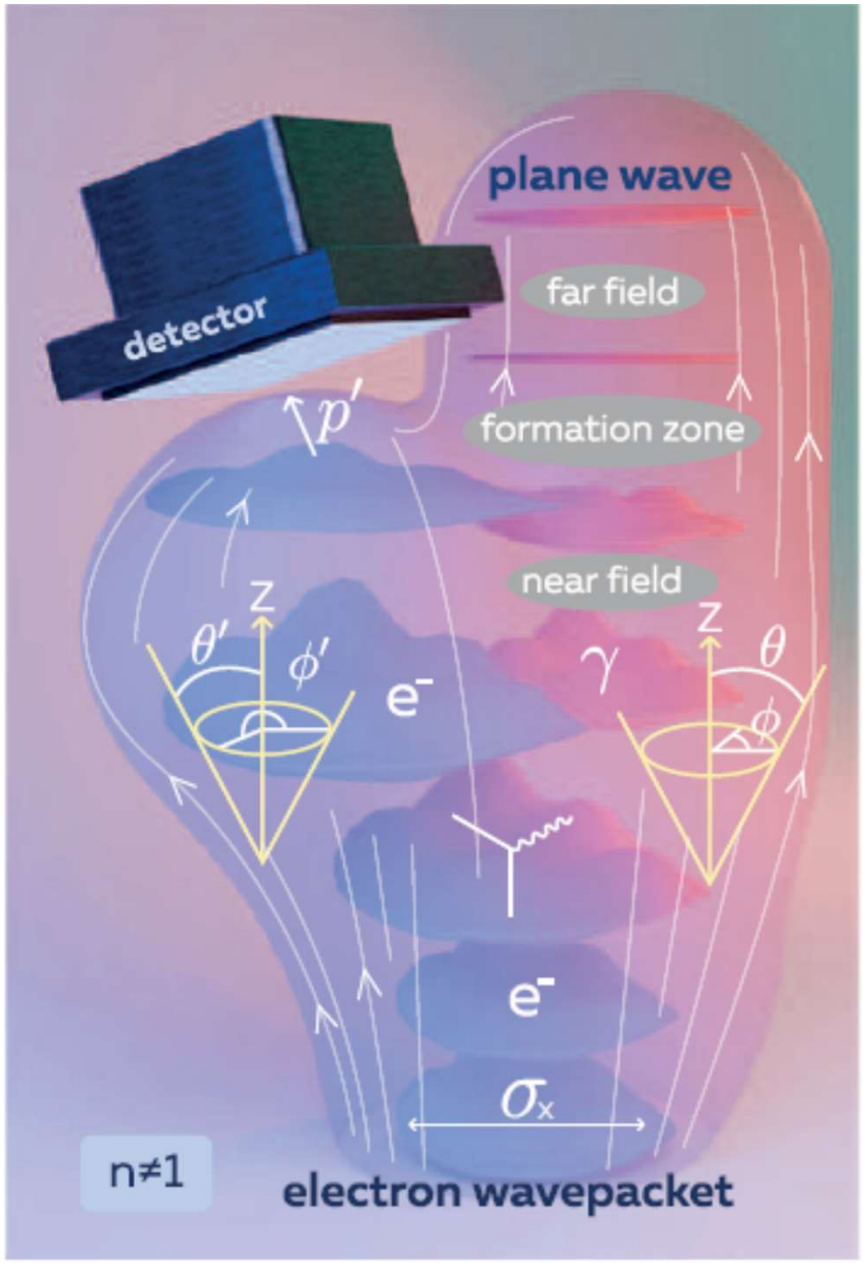

1. Spreading time of the photon field

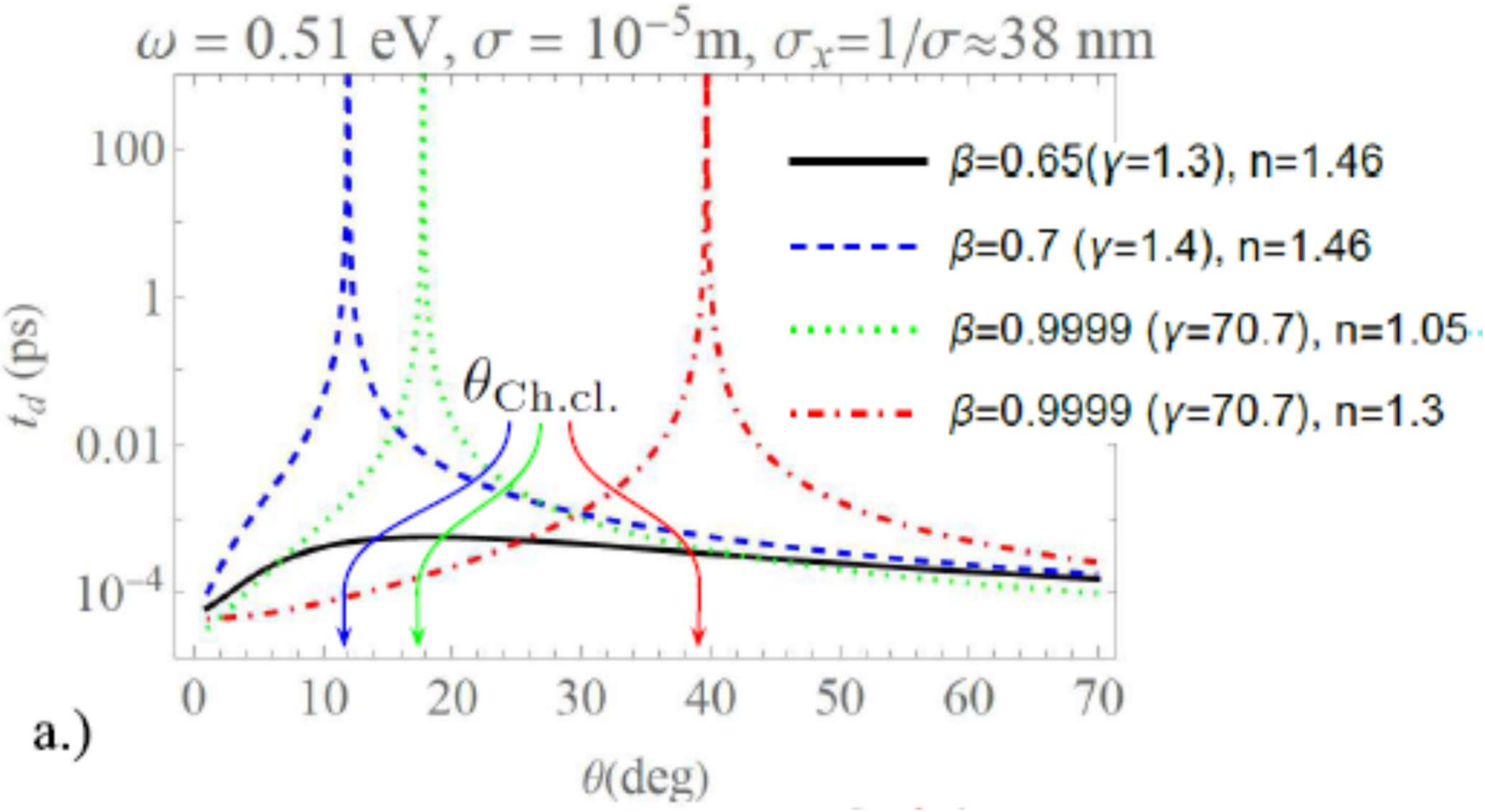

The spreading time turns negative
nearby the classical Cherenkov angle due to the quantum recoil

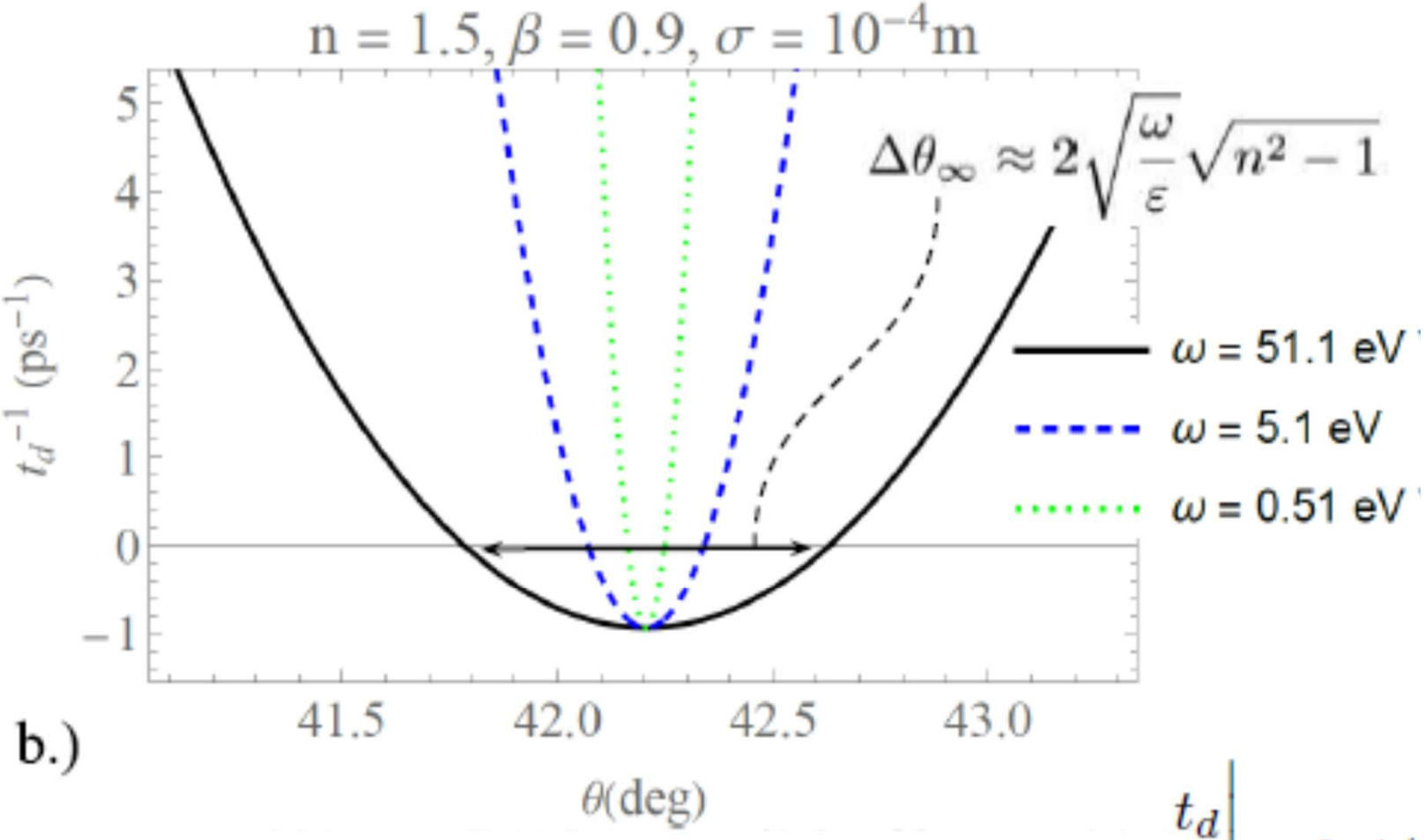

The spreading time of the electron packet itself!

$$t_d\Big|_{\cos\theta=1/nu_p} = \frac{2\varepsilon}{\sigma^2}\frac{n^2}{1-n^2} < 0,$$

2. The Mach cone shows the photon near-field,
a.k.a. the wake-field

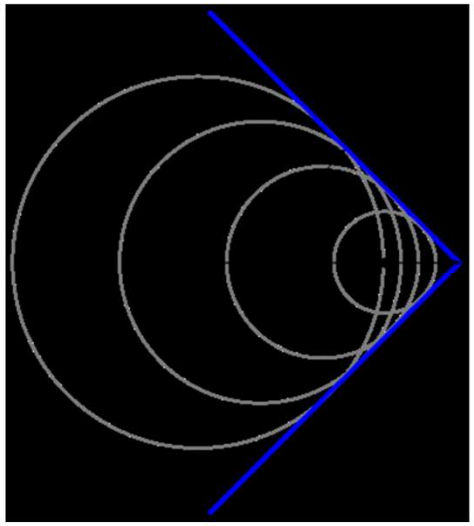

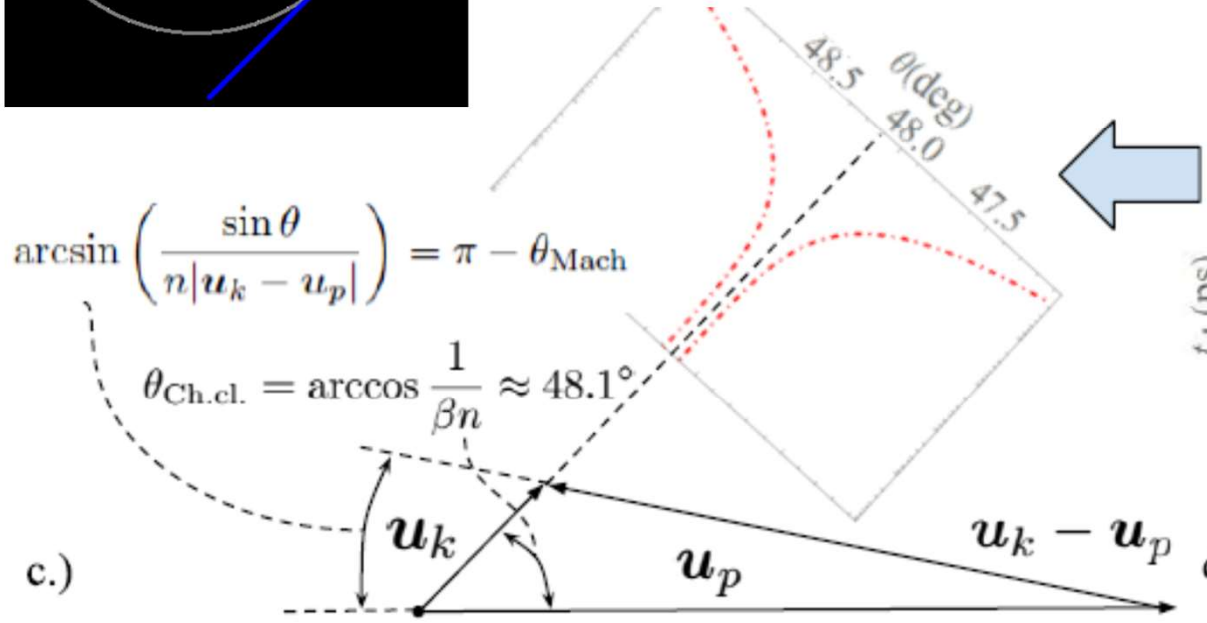

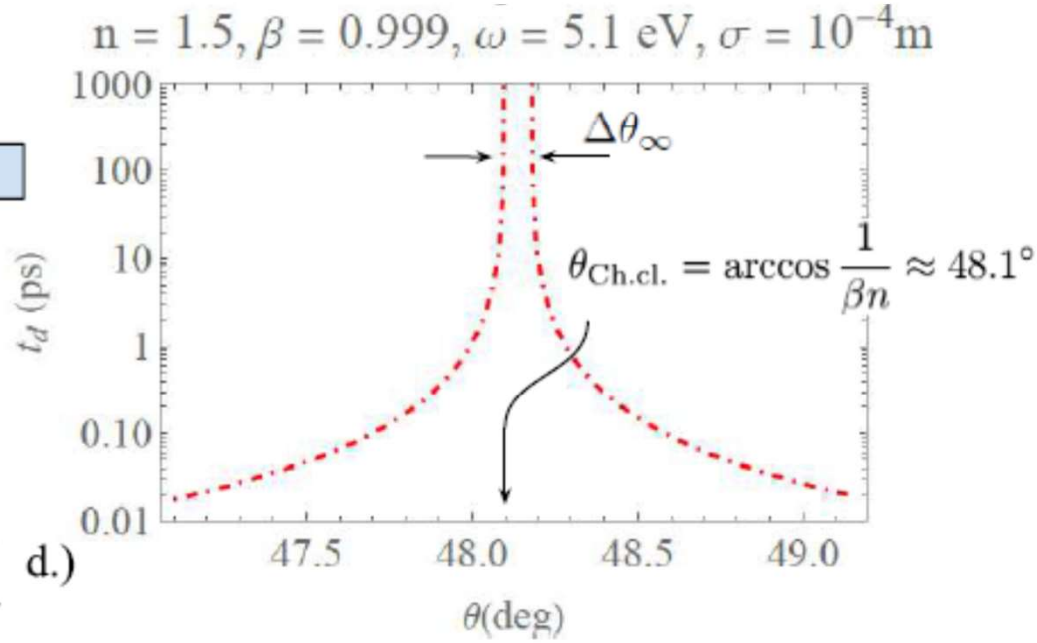

2. The Mach cone shows the photon near-field, a.k.a. the wake-field

$$\mathcal{W}(\mathbf{r},\mathbf{k},t) \propto \int_0^\infty dt' \, \frac{e^{-R^2/R_{\rm eff}^2(t')}}{G(t')} \cos\left(F(t')\right),$$

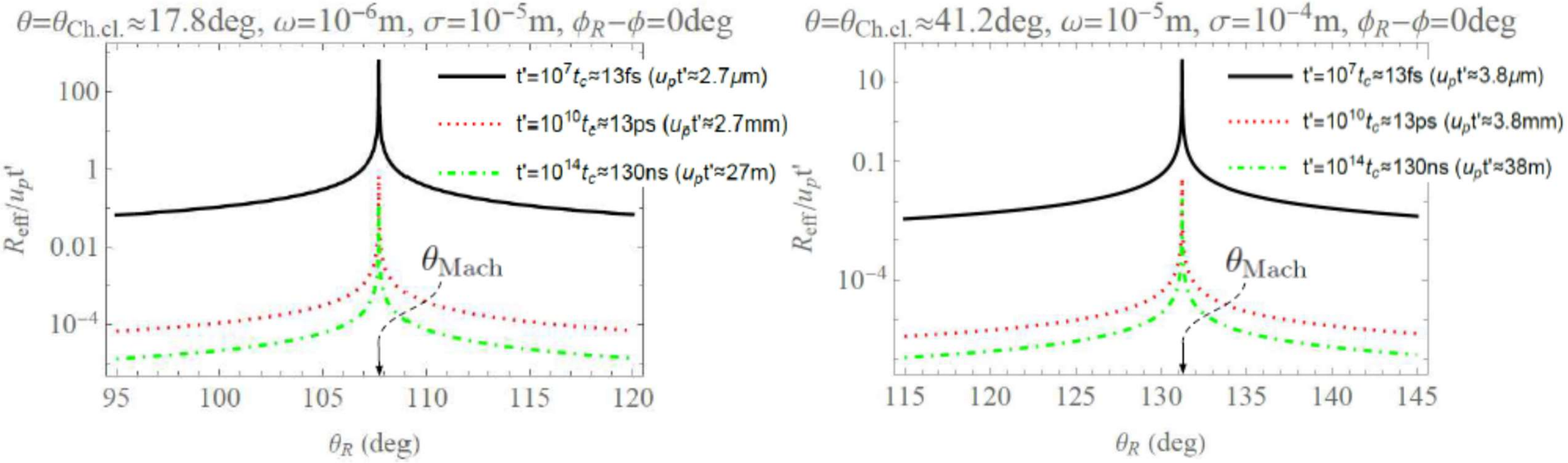

Figure 2: The effective correlation radius from Eq.(7) divided by the distance $u_p t'$ traveled by the electron during the time t'. Left: $\beta = 0.7\,(\gamma = 1.4), n = 1.5$, $\theta_{\rm Ch.cl.} = \arccos 1/u_p n \approx 17.8$ deg, $\theta_{\rm Mach} \approx 107.8$ deg. Right: $\beta = 0.9999\,(\gamma = 70.7), n = 1.33$, $\theta_{\rm Ch.cl.} \approx 41.2$ deg, $\theta_{\rm Mach} \approx 131.2$ deg. Nearby the Mach angle, space-time dependence of the Wigner function quickly vanishes within the correlation radius $R < R_{\rm eff}(t')$.

3. The photon arrival time

Classically, a photon generated at *r=0, t=0* arrives at the point detector at

$$t_{\text{cl.}}^{(\text{far-f.})} = r/u_k = r\,n,$$

In our QFT approach:

$$\exp\left\{-\frac{R^2}{R_{\text{eff}}^2(t')}\right\} \propto \exp\left\{-\frac{(t-t_0)^2}{2\sigma_t^2(t')}\right\},$$

$$t_0 = l_0 \cdot (\mathbf{r} + (\partial_{\mathbf{p}} + \partial_{\mathbf{k}})\zeta_{fi}) \qquad l_0 = [(u_p - u_k) \times [u_k \times u_p]] \,/\, [u_p \times u_k]^2$$

The shift from the classical arrival time is due to the phase:

$$\Delta t = t_0 - t_{\text{cl.}} = l_0 \cdot (\partial_{\mathbf{p}} + \partial_{\mathbf{k}})\zeta_{fi}$$

3. The photon arrival time

The width of the distribution

$$\exp\left\{-\frac{R^2}{R_{\rm eff}^2(t')}\right\} \propto \exp\left\{-\frac{(t-t_0)^2}{2\sigma_t^2(t')}\right\},$$

defines the Cherenkov flash duration

$$\sigma_t^2(t') = \frac{\sigma_x^2(t')}{2}\frac{(\boldsymbol{u}_p - \boldsymbol{u}_k)^2}{[\boldsymbol{u}_p \times \boldsymbol{u}_k]^2}$$

The length of the electron packet

$$\sigma_x^2(t') = \sigma^{-2}\left(1 + (t'/t_d)^2\right)$$

Nearby the classical Cherenkov angle:

$$\sigma_t(t') \to n\,\sigma_x(0)/\sqrt{2},$$

$$\sigma_x(0) \sim 1 - 100\,\text{nm} \longrightarrow \sigma_t(0) \sim 10\,\text{as} - 1\,\text{fs}$$

The first classical estimate by I.M. Frank yielded < 1 ps,
Uspekhi Fiz. Nauk [Sov. Phys. Usp.] 58, 111 (1956), (in Russian).

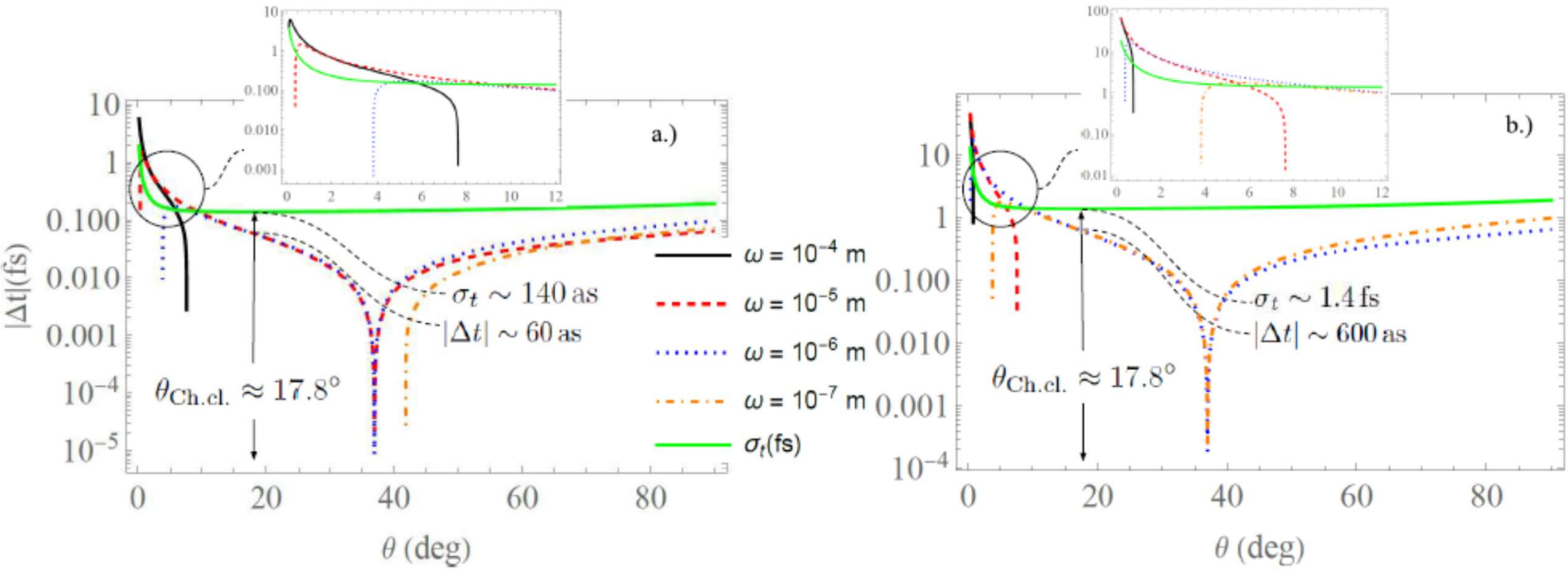

Figure 4: The quantum shift $\Delta t = t_0 - t_{\text{cl.}} = \boldsymbol{l}_0 \cdot (\partial_{\mathbf{p}} + \partial_{\mathbf{k}})\zeta_{fi}$ from Eq.(15) of the photon arrival time compared to the classical value and the Cherenkov flash duration (the green lines with $\sigma = p_\perp$). The electron energy is typical for a transmission electron microscope: $\beta = 0.7$, and $p'_\perp = 0.99 \times p_\perp, p'_z = 0.9 \times \beta, n = 1.5$. The left panel (a.): $p_\perp = 10^{-5}\, m$, $1/p_\perp \gtrsim 10\,\text{nm}$, the right panel (b.): $p_\perp = 10^{-6}\, m$, $1/p_\perp \gtrsim 100\,\text{nm}$. The behaviour at small angles is shown in the insets. The shifts vanish in those regions that are not allowed by the momentum conservation law, they stay roughly the same for other $p'_\perp, p'_z$ and for ultrarelativistic electrons, $\gamma \gg 1$, though the Cherenkov angle grows.

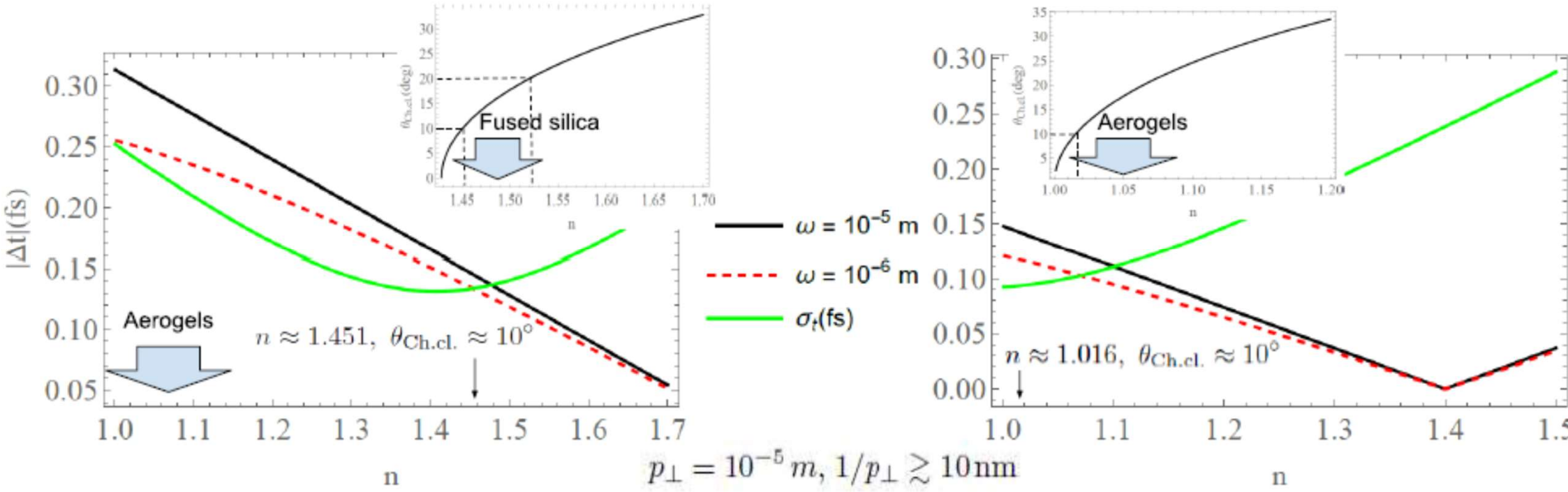

Figure 5: Dependence of the shift $\Delta t = t_0 - t_{\text{cl.}} = l_0 \cdot (\partial_{\mathbf{p}} + \partial_{\mathbf{k}})\zeta_{fi}$ from Eq.(15) of the photon arrival time on the refractive index n at the emission angle $\theta = 10$ deg. Left: $\beta = 0.7, p'_z = 0.9 \times \beta$ (a TEM regime; the minimal refractive index for which the Cherenkov condition is met is $n \approx 1.429$, whereas $n = 1.45 - 1.55$ for fused silica in the given spectral range), right: $\beta = 0.9999(\gamma = 70.7), p'_z = 0.99 \times \beta$ (an accelerator regime). The classical Cherenkov angle $\theta_{\text{Ch.cl.}} = \arccos 1/\beta n$ is shown in the insets.

4. Summary and Outlook

- The R-t approach allows us to study much reacher physics
- We describe the formation of Cherenkov radiation in real space and time
- The photon Wigner function is not everywhere-positive, so such quantum-optical techniques as tomography and the Radon transform can come in handy
- The attosecond time scales hint to microscopic (atomic) physics. It has two origins:
  1. The size of the electron packet: ~ 1 nm → attoseconds,
  2. The finite frequency interval contributing to the field: this interval^-1 defines a time uncertainty in the photon arrival time, exactly as in the AC-Stark effect
- Nm-sized electron packets with no spreading → attosecond photon flashes
- Nm-sized vortex electron packets can produce attosecond twisted Cherenkov photons
- The quantum shift of the photon arrival time can be observed nearby the Cherenkov angle

https://arxiv.org/abs/2411.00212

department of PHYSICS

Thank you
and special thanks to my group!

https://arxiv.org/abs/2411.00212

d.karlovets@gmail.com
https://physics.itmo.ru/ru/research-group/5430

If the electron is a plane wave:

$$\delta(\mathbf{p}'_\perp + \mathbf{k}_\perp) = \delta(p'_x + k_x)\delta(p'_y + k_y) = \frac{1}{p'_\perp}\,\delta(p'_\perp - k_\perp)\left(\delta(\phi' - (\phi_k - \pi))\Big|_{\phi_k \in [\pi, 2\pi]} + \delta(\phi' - (\phi_k + \pi))\Big|_{\phi_k \in [0,\pi]}\right)$$

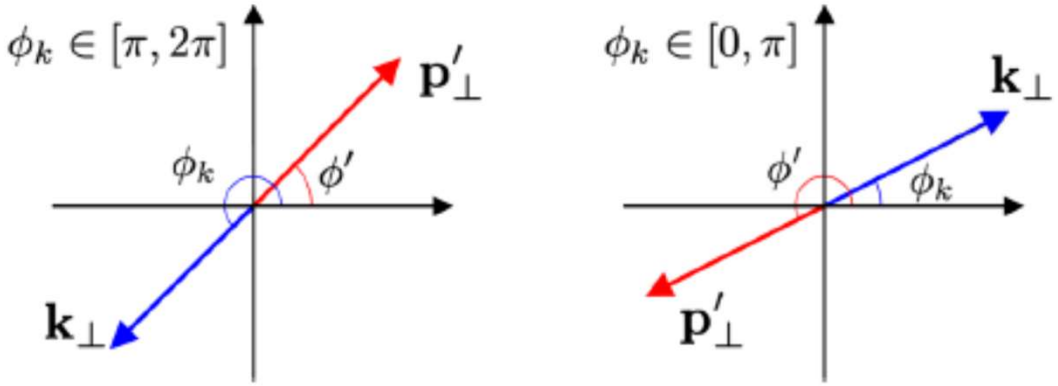

$$|\gamma\rangle = \langle f_e^{(\mathrm{det})}|e_{\mathrm{in}}\rangle|0_\gamma\rangle + \sum_{\lambda',\lambda_\gamma}\int \frac{d^3k}{(2\pi)^3}\frac{d^3p'}{(2\pi)^3}\,|\mathbf{k},\lambda_\gamma\rangle\,(f_e^{(\mathrm{det})}(\mathbf{p}',\lambda'))^*\,S_{fi}^{(1)},$$

3 delta-functions 4 delta-functions

The photon evolved state is a plane wave!

If the final electron is not detected:

$$\sum_{\lambda'} \int \frac{d^3p'}{(2\pi)^3} \frac{1}{4\pi} \left| \langle 0|\hat{\boldsymbol{E}}(\boldsymbol{r},t)|\gamma\rangle \right|^2 = \sum_{\lambda'} \int \frac{d^3p'}{(2\pi)^3} \frac{d^3k}{(2\pi)^3} \mathcal{W}(\mathbf{r},\mathbf{k},t) =$$

$$= \sum_{\lambda'} \int \frac{d^3p}{(2\pi)^3} \frac{d^3k}{(2\pi)^3} \mathcal{W}_p(\mathbf{r},\mathbf{p},\mathbf{k},t)\Big|_{\mathbf{p}'=\mathbf{p}-\mathbf{k}}.$$

On the way to experiments at accelerators….

The project of the relativistic vortex electron source at Joint Institute for Nuclear research (Dubna):

- First at a 6-MeV electron photo-gun,
- Then at the 200-MeV linac

https://rscf.ru/en/project/23-62-10026/